Earth and Planetary Science Letters, 34 (1977) 300–306

[5]

ELASTICITY OF SINGLE-CRYSTAL MgF_2 (RUTILE STRUCTURE) UNDER PRESSURE

GEOFFREY F. DAVIES [1]

Hoffman Laboratory, Harvard University, Cambridge, Mass. 02138 (USA)

Received October 4, 1976
Revised version received November 29, 1976

The elastic moduli of single-crystal MgF_2 (rutile structure) have been measured ultrasonically to 7 kbars. Zero-pressure moduli are in good agreement with the results of others. The pressure derivative of the shear modulus $c_s = (c_{11} - c_{12})/2$ is -0.7 ± 0.1 which is consistent with the negative values also found in rutile-structure oxides. Estimates of the isotropic aggregate modulus derivatives are in good agreement with derivatives measured on polycrystalline aggregates by Rai and Manghnani. The calculated isotropic aggregate bulk modulus derivative is $K' = 5.1 \pm 0.2$, which is lower than for the rutile-structure oxides, and comparable to that for other fluorides. More covalent bonding may increase the value of K', and hence the value for stishovite (SiO_2, rutile) may be quite high.

1. Introduction

The elastic properties of materials with the rutile crystal structure are of particular interest in geophysics because of the existence of stishovite, the high-pressure rutile-structure phase of SiO_2 [1]. Stishovite may exist as a stable phase in all or part of the lower mantle [2,3]. In any case, its density and elastic properties are important reference data for estimating the properties of possible mantle mineral assemblages and for interpreting the density and elastic velocity profiles of the mantle [4,5]. Because of the difficulty of making or collecting sufficient quantities of stishovite, even its zero-pressure eleastic properties are still quite uncertain [6–9], and shock wave data for silica do not provide very strong constraints [10,11].

To date, the single-crystal elastic properties of three other rutile-structure oxides have been measured under pressure (Table 1); rutile itself (TiO_2), GeO_2, and cassiterite (SnO_2). Two notable features of the results are the unusually large-pressure derivatives of the bulk modulus, K' (compared with "usual" values of 4–5), and the negative pressure derivatives of one shear mode, c_s'. In trying to infer from these results the likely properties of stishovite, it would be useful to know to what extent the properties are intrinsic characteristics of the crystal structure, and to what extent they depend on the character of the interatomic bonding (ionic vs. covalent) or the character of the metals (transition vs. group IV). The pattern of relative magnitudes of the elastic moduli of rutile is in fact slightly different than that of the other two, indicating that the transition character of Ti has some influence. Transition metals are also associated with anomalous elastic properties in other compounds [5].

An indication of the influence of bond character on the elastic properties can be obtained from a comparison of the oxides with fluorides which crystallize in the rutile structure, since the latter should be more ionic. Zero-pressure single-crystal elastic moduli have been measured for MgF_2, MnF_2 and CoF_2 (see Table 1), but no measurements of single-crystal properties under pressure have been reported to date. Recently the pressure dependence of the elastic moduli of polycrystalline MgF_2 have been reported by Rai and Manghnani [12]. Measurements of the single-crystal moduli under pressure are still desirable because they

[1] Present address: Department of Geological Sciences, The University of Rochester, Rochester, N.Y. 14627, U.S.A.

TABLE 1

Single-crystal elastic moduli, c_{ij} (Mbars), and their pressure derivatives c'_{ij}, of rutile-structure compounds, (bulk moduli, K, and shear moduli, μ, of isotropic aggregates are estimated from the Hashin-Shtrikman bounds [26,27])

	c_{11}	c_{33}	c_{12}	c_{13}	c_{44}	c_{66}	c_s *	K	μ	Reference
GeO_2	3.372	5.994	1.882	1.874	1.615	2.584	0.745	2.58	1.51	[33]
TiO_2	2.714	4.840	1.780	1.496	1.244	1.948	0.467	2.15	1.14	[34]
	2.701	4.819	1.766	1.480	1.239	1.930	0.468	2.13	1.13	[30]
SnO_2	2.617	4.496	1.772	1.555	1.031	2.074	0.423	2.12	1.02	[35]
MnF_2	1.030	1.628	0.816	0.709	0.300	0.677	0.107	0.893	0.30	[22]
CoF_2	1.023	1.704	0.730	0.610	0.373	0.952	0.147	0.836	0.39	[36]
MgF_2	1.237	1.770	0.732	0.536	0.552	0.978	0.253	0.868	0.52	[25]
	1.395	2.041	0.897	0.625	0.564	0.951	0.250	1.010	0.54	[23]
	1.399	2.042	0.893	0.637	0.570	0.954	0.253	1.014	0.55	[22]
	1.408	2.053	0.900	0.635	0.567	0.957	0.254	1.019	0.55	[24]
	1.427	2.040	0.922	0.641	0.567	0.935	0.253	1.028	0.55	this paper **
	±0.003	±0.005	±0.005	±0.010	±0.002	±0.015	±0.001	±0.010	±0.01	
	c'_{11}	c'_{33}	c'_{12}	c'_{13}	c'_{44}	c'_{66}	c'_s	K'	μ'	Reference
GeO_2	6.65	6.63	8.05	4.10	1.78	4.10	−0.70	6.1	1.13–1.59	[33]
TiO_2	6.47	8.34	9.10	5.02	1.10	6.43	−1.32	6.8	0.50–1.34	[34]
	6.29	8.13	9.02	5.57	1.08	5.91	−1.37	6.9	0.35–1.16	[30]
SnO_2	5.25	6.10	6.73	4.65	0.89	3.18	−0.74	5.5	0.28–0.76	[35]
MgF_2	5.0	5.7	6.4	4.2	0.8	2.9	−0.7	5.1	0.38–0.72	this paper ***
	±0.1	±0.1	±0.2	±0.3	±0.1	±0.2	±0.1	±0.2		
	–	–	–	–	–	–	–	5.1 ‡	0.7 ‡	[12]
	(3.31)	(3.96)	(5.21)	(3.31)	(−0.31)	(2.94)	(−0.95)	(3.84)	(−0.25–0.11)	[31] ‡‡

* $c_s = 1/2(c_{11} - c_{12})$.
** Uncertainties derived from deviations from internal consistency (Table 3).
*** Uncertainties derived from scatter in data.
‡ Measurements on polycrystalline aggregates.
‡‡ Values in parentheses are theoretical.

provide more information on the nature of the interatomic forces, and because the reliability of measurements on polycrystals has been questioned (e.g. [13]). This paper reports the results of ultrasonic measurements of the elastic moduli of single-crystal MgF_2 under pressures up to 7 kbars. These results are less accurate than is commonly achieved (or claimed) in ultrasonic measurements, but they are nevertheless accurate enough to be useful.

2. Specimens

Five crystals of MgF_2, with the orientations listed in Table 2, were purchased from Optovac Inc., North Brookfield, Mass., each being about 1 cm long and 1 cm in diameter. One pair of faces, flat and parallel to within about 1 μm, was polished on each crystal by Valpey-Fisher Corporation. The orientations of the faces were checked by Laue X-ray back-reflection, and found to be within 1° of those listed, except for specimen 5, which was misaligned by 6°. A rough estimate indicates that this error will not affect the results within the accuracy reported here. The final lengths of the samples are listed in Table 2.

MgF_2 (rutile) has tetragonal symmetry (space group D^{14}_{4h}–$P4/mmm$), and consequently has six independent second-order elastic moduli [14]. The combinations of these moduli which control the velocities of compressional and shear waves in the crystallographic orientations of the above specimens are listed in Table 2. The eleven modes of propagation are sufficient to determine all six independent moduli with some redundancy.

TABLE 2

Crystal lengths, wave modes and corresponding combinations of elastic moduli for MgF_2 samples

Length (cm)	Mode	Mode *	Modulus
Crystals 1 and 2			
1.0797	1	[001]L	c_{33}
	2	[001]T any	c_{44}
Crystal 3			
0.9639	3	[100]L	c_{11}
	4	[100]T[010]	c_{66}
	5	[100]T[001]	c_{44}
Crystal 4			
1.0797	6	[110]L	$c_L = \frac{1}{2}(c_{11} + c_{12} + 2c_{66})$
	7	[110]T[1$\bar{1}$0]	$c_T = \frac{1}{2}(c_{11} - c_{12})$
	8	[110]T[001]	c_{44}
Crystal 5			
0.9639	9	45°L **	$c_{QL} = \frac{1}{4}(A + B)$ ***
	10	45°T45° **	$c_{QT} = \frac{1}{4}(A - B)$ ***
	11	45°T[010] **	$\frac{1}{2}(c_{44} + c_{66})$

* Wave normal direction, type (longitudinal, L, or transverse, T) and polarization.

** Wave normal 45° to [100] and [001].

*** $A = c_{11} + c_{33} + 2c_{44}$, $B = [(c_{11} - c_{33})^2 + 4(c_{13} + c_{44})^2]^{1/2}$. Modes 9 and 10 are not purely longitudinal and transverse, respectively.

3. Experimental methods

Ultrasonic measurements were made using an interferometer system, described in detail by R.J. O'Connell et al. (in preparation) and basically similar to that described by Spetzler [15]. Two high-frequency phase coherent ultrasonic pulses are generated in the sample via quartz transducers, the second pulse superimposed on the echo of the first. Variation of the ultrasonic frequency produces alternate constructive and destructive interference, which is monitored via the amplitude of a selected echo combination. The phase of the interference cycle is directly related to the phase difference between the pulses, and hence to the sound velocity, and is determined as a function of frequency via a series of Fourier transform algorithms. An on-line mini-computer controls the data acquisition and performs the initial data processing. Pressure derivatives were here calculated from a determination of the variation of phase with pressure at a fixed frequency. Used in this way, the method is therefore equivalent to the widely used pulse superposition method described by McSkimin and Andreatch [16].

Pressures up to 7 kbars were generated with a Bridgman piston-cylinder apparatus with a kerosene pressure medium. Pressure was determined to within 1% with a Heise gauge.

Measurements of zero-pressure velocities were made with a steel buffer rod between the transducer and sample. The buffer rod and sample were bonded with phenyl salicylate, which melts at 44°C, and hence can easily be made to form a thin bond. 20 MHz transducers were used, and phase was measured between about 10 and 30 MHz. The phase difference between successive echoes is:

$$\phi = \frac{4\pi f L}{v} + \phi_r \qquad (1)$$

where f is the ultrasonic frequency, L is the sample length, v is the wave velocity and ϕ_r is the phase shift due to reflections at the ends of the sample. A constant phase shift of π occurs at the free end. The buffer-sample bond causes a phase shift at the buffer end of the sample which depends on frequency. This type of phase shift has been investigated theoretically and experimentally by McSkimin [17,18] and Davies and O'Connell [19]. The results of Davies and O'Connell indicate that $d\phi_r/df$ is likely to be less than about 0.1% of $d\phi/df$. The effects of the bond phase shift can thus be ignored to this accuracy. In terms of the frequency step $\Delta f = 2\pi/(d\phi/df)$ between successive constructive interferences, the velocity is, from equation (1):

$$v = \frac{4\pi L}{d\phi/df} = 2L\Delta f \qquad (2)$$

Δf is the reciprocal of the round-trip travel time of the wave through the sample.

Measurements under pressure were made with transducer bonded directly onto the sample with Dow Chemical resin 276-V9. Both the transducer and the bond cause a phase shift upon reflection from that face of the sample. The bond phase shift is very small at the

resonance frequency, f_r, of the transducer [16]. It increases away from the resonance frequency, but decreases with increasing pressure [19]. The transducer phase shift varies in a predictable way with frequency [20], and the variation of f_r with pressure has been measured [21]. By determining the phase as a function of pressure at the zero-pressure resonance frequency, f_{r0}, and correcting for the transducer phase shift, the effect of the bond phase shift on the measured pressure derivative of the relevant elastic modulus should amount to less than 0.02 [19]. The relevant combination of elastic moduli is $M = \rho v^2$, where ρ is the density. Expressions for the pressure derivative of M and for the transducer correction are [19]:

$$\frac{\partial M}{\partial P} = -2\frac{M}{\phi}\frac{\partial \phi}{\partial P} + \frac{M}{K_T}(1 - 2K_T\beta_T) + \left(\frac{\partial M}{\partial P}\right)_{corr.} \quad (3)$$

$$\left(\frac{\partial M}{\partial P}\right)_{corr.} = \frac{v^2}{L}\frac{Z_t}{f_r}\frac{\partial \ln f_r}{P} \quad (4)$$

where $K_T = \rho(\partial P/\partial \rho)_T$ is the isothermal bulk modulus and $\beta_T = -(\partial \ln L/\partial P)_T$ is the linear compressibility of the sample, and $Z_t = \rho_t v_t$ is the transducer impedance. Expressions for the linear compressibility of tetragonal crystals in any direction, in terms of the elastic compliances or stiffnesses, are given by Nye [14]. Equation (3) contains implicitly the correction for the change in length of the crystal under pressure.

4. Zero-pressure results

The results of the zero-pressure measurements are given in Table 3 in terms of the pseudo-resonance frequency, Δf, of the path, along with the derived elastic wave velocity and corresponding modulus. The X-ray density of 3.178 g/cm^3 [22] was assumed.

The six independent elastic moduli where determined from the eleven mode moduli by requiring a simultaneous least-squares fit to the mode moduli. The resulting best-fit moduli are included in Table 1. The internal consistency of the data is demonstrated by the comparison, in Table 3, of the measured mode moduli with those recalculated from the set of best-fit moduli. The discrepancies of all but modes 10 and 11 are less than 0.3%. Modes 9 and 10 may have been affected by the fact that they are not pure longitudinal and transverse, respectively, so that coupling of modes can occur at reflections. For all modes, an internal consistency within 1% of the mode moduli is assured.

TABLE 3

Measured pseudo-resonance frequencies, velocities and corresponding moduli of various modes in MgF_2 at zero pressure. Mode moduli calculated from best-fit c_{ij} (Table 1) are included to show internal consistency

Crystal	Mode	Δf (kHz)	v (km/s)	$M = \rho v^2$ (Mbars)	M (best-fit c_{ij}) (Mbars)	Discrepancy (%)
1	1	370.7	8.005	2.037	2.040	0.2
	2	195.6	4.224	0.567	0.567	0
2	1	371.5	8.023	2.045	2.040	0.3
	2	195.4	4.220	0.566	0.567	0.2
3	3	347.7	6.703	1.428	1.427	0.1
	4	281.1	5.418	0.933	0.935	0.2
	5	218.9	4.220	0.566	0.567	0.2
4	6	377.2	8.146	2.109	2.110	0.1
	7	130.5	2.818	0.252	0.2525	0.2
	8	195.4	4.220	0.566	0.567	0.2
5	9	387.2	7.465	1.771	1.773	0.1
	10	210.9	4.066	0.525	0.527	0.4
	11	253.1	4.879	0.757	0.751	0.9

The six independent moduli are compared with other measurements of MgF_2 in Table 1. The uncertainties given in Table 1 are derived from the deviations from internal consistency (Table 3). Discrepancies between the present results and those of Haussühl [22], Aleksandrov et al. [23] and Jones [24] are somewhat larger: 3% for c_{12} (errors are compounded in deriving this from the measured moduli; see Table 2), and up to 2% for the other moduli. Thus the present data are in quite good agreement with some other recent measurements, although the discrepancies are larger than would be expected from the internal consistency of the data (as is commonly found in ultrasonic measurements). In contrast, the results of Cutler et al. [25] differ from the others by more than 10% in some cases.

5. Pressure derivatives

The measurements of relative phase vs. pressure are illustrated in Fig. 1. Only two of the runs were completed to 7 kbars because of various difficulties. Modes 1, 2, 7 and 8 terminated because the bond deteriorated and the signal was lost. In the initial runs with crystals 1 and 2, the crystals were cracked around the transducer by too rapid decompression (presumably because of differential expansion of the transducer and the sample), in the first case because of a broken seal, and in the second from inexperience. The mode 2 data may be affected by this cracking. The modes 7 and 8 data are not of high quality, be-

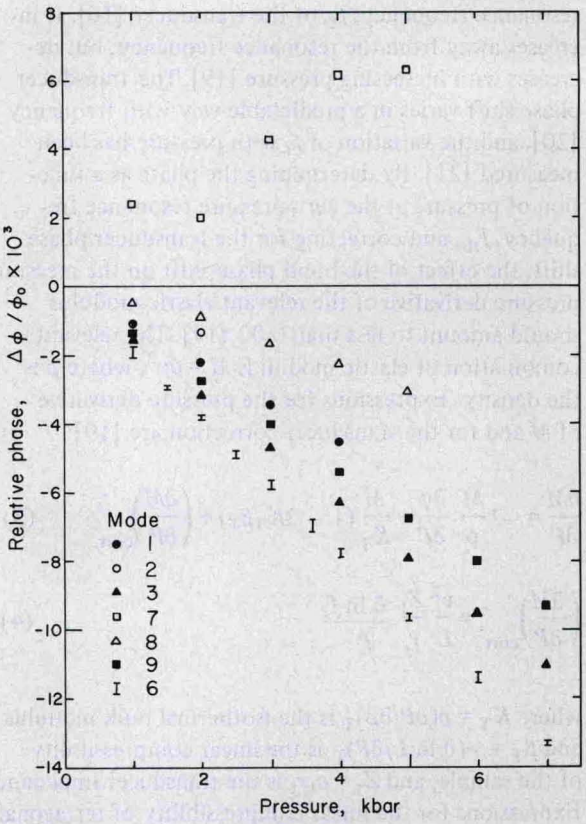

Fig. 1. Measured relative phase increment vs. pressure for indicated modes (Table 2) of MgF_2. Mode 6 data are converted from measurements of frequency shift vs. pressure, using $(\partial \ln \phi/\partial P)_f = -(\partial \ln f/\partial P)_\phi$, without any transducer correction, which is very small in this case. Bars denote results for adjacent constructive and destructive interferences which bracketed the transducer resonance frequency.

TABLE 4

Measure pressure derivatives of phase, and derived pressure derivatives of mode moduli

Mode	$\partial\phi/\partial P$ * (rad/kbar)	$(1/K) - 2\beta$ (Mbar^{-1})	f_r (MHz)	$(\partial M/\partial P)_{corr.}$	$\partial M/\partial P$
1	−0.39 ± 0.01	0.44	20	0.07	5.66 ± 0.15
2	−0.41	0.44	20	−0.03	0.94
3	−0.86 ± 0.01	0.27	10	0.10	5.01 ± 0.06
6	−0.93 ± 0.015 **	0.27	10	0.14	8.59 ± 0.14
7	1.4 ± 0.1	0.27	20	−0.02	−0.68 ± 0.05
8	−0.38 ± 0.05	0.27	20	−0.03	0.79 ± 0.10
9	−0.65 ± 0.01	0.35	10	0.13	5.51 ± 0.08

* Uncertainties estimated from scatter in data (Fig. 1).
** Calculated from measurement of $\partial f/\partial P$.

cause coupling of the two modes by the transducer at each reflection resulted in some mutual contamination. The mode 6 data were obtained by manual measurements of the frequency shift of the interference pattern because the on-line computer had failed. In spite of the incompleteness and poor quality of some of the data, they are sufficient to constrain the moduli derivatives fairly well because none of the larger relative errors (such as in mode 7, Fig. 1) were translated into large absolute errors.

The measured phase derivatives, with uncertainties estimated from the scatter in the data, are given in Table 4, along with the derived mode moduli derivatives, including corrections for length change and transducer phase shift. The transducer longitudinal and transverse impedances are 15.2 and 10.3×10^5 g cm^{-2} s^{-1}, respectively, and the logarithmic resonance frequency derivatives are 1.51 and -3.68 Mbar^{-1} [21]. The only redundancy in these data is between modes 2 and 8. Since mode 2 is suspect, the mode 8 data were used, with fairly large uncertainty. The measured and derived single crystal moduli derivatives are included in Table 1. The estimated uncertainty of the derived quantities is about 0.2–0.3, based on the uncertainties of the measured derivatives given in Table 4.

Pressure derivatives of the isotropic aggregate bulk and shear moduli are also included in Table 1. These have been estimated from the derivatives of the Hashin-Shtrikman bounds [26,27], but it should be noted that these are not themselves bounds on the derivatives. It can be seen that the estimates of the shear modulus derivative are quite uncertain. The estimated isotropic aggregate derivatives are compared in Table 1 with measured derivatives on polycrystalline aggregates given by Rai and Manghnani [12]. The agreement is excellent.

6. Discusssion

These results suggest that the two most notable features of the pressure derivatives of the elastic moduli of the rutile-structure oxides are also present in this fluoride analogue: the value of K' of 5.1 is fairly high, though not as high as in any of the oxides, and the value of $c'_s = (c'_{11} - c'_{12})/2$ is negative.

The value of K' may not in fact be unusually high for fluorides. The values of K' for LiF, NaF, KF (rocksalt structures) and CaF_2 and BaF_2 (fluorite structures) all are in the range 4.9–5.2 [5]. The increasing values of K' through the sequence MgF_2, SnO_2, GeO_2 suggest that larger values of K' may be associated with more covalent bonding. Thus stishovite may indeed have a quite high value of K', close to 7 [5].

The long wavelength B_{1g} optic mode of rutile also has a negative pressure derivative [28,29]. It has been pointed out that the combined displacements associated with the B_{1g} optic mode and the c_s acoustic mode are the same as those required to transform the rutile structure into the $CaCl_2$ structure [30]. Both of these "mode softenings"may thus be associated with an approaching instability of the rutile structure.

Theoretical predictions of the pressure derivatives of the elastic moduli were made by Striefler and Barsch [31] using a modified rigid-ion model including an effective ionic charge and first- and second-nearest neighbor central repulsive forces of the Born-Mayer type. Their predicted values are included in Table 1, and can be seen to be consistently substantially lower than the measured values. In analogous models of rutile-structure oxides, Striefler and Barsch [32] found that non-central forces had to be included in order to obtain a reasonable fit to data. The discrepancies for MgF_2 suggest that some such modification of the model is also required in the case of fluorides.

Acknowledgement

I am grateful to R.J. O'Connell for discussions, assistance, and the use of laboratory facilities.

This research was supported by the Committee on Experimental Geology and Geophysics of Harvard University by National Science Foundation grant GA 38899 (Earth Sciences).

References

1 S.M. Stishov and S.V. Popova, A new dense modification of silica, Geokhimya 10 (1961) 923.

2 L. Ming and W.A. Bassett, High-pressure phase transformations in the system $MgSiO_3$–$FeSiO_3$, Earth Planet. Sci. Lett. 27 (1975) 85.

3 L.G. Liu, Post-oxide phases of forsterite and enstatite, Geophys. Res. Lett. 2 (1975) 417.
4 G.F. Davies, Limits on the constitution of the lower mantle, Geophys. J.R. Astron. Soc. 38 (1974) 479.
5 G.F. Davies, The estimation of elastic properties from analogue compounds, Geophys. J.R. Astron. Soc. 44 (1976) 625.
6 H. Mizutani, Y. Hamano and S. Akimoto, Elastic-wave velocities of polycrystalline stishovite J. Geophys. Res. 77 (1972) 3744.
7 R.C. Liebermann, A.E. Ringwood and A. Major, Elasticity of polycrystalline stishovite, Earth Planet. Sci. Lett. 32 (1976) 127.
8 B. Olinger, The compression of stishovite, J. Geophys. Res. 81 (1976) 5341.
9 Y. Sato, Equation of state of mantle minerals determined through high-pressure X-ray study, in: High Pressure Research: Applications in Geophysics, M.H. Manghnani and S. Akomoto, eds. (Academic Press, New York, N.Y., 1977).
10 G.F. Davies, Equations of state and phase equilibria of stishovite and a coesitelike phase from shock-wave and other data, J. Geophys. Res. 77 (1972) 4920.
11 E.K. Graham, On the compression of stishovite, Geophys J.R. Astron. Soc. 32 (1973) 15.
12 C.S. Rai and M.H. Manghnani, Pressure and temperature dependence of the elastic moduli of polycrystalline stishovite, J. Am. Ceram. Soc. 59 (1976) 499.
13 H.A. Spetzler, E. Schreiber and R.J. O'Connell, Effect of stress-induced anisotropy and porosity on elastic properties of polycrystals, J. Geophys. Res. 77 (1972) 4938.
14 J.F. Nye, Physical Properties of Crystals (Oxford Univ. Press, Oxford, 1957),
15 H. Spetzler, Equation of state of polycrystalline and single-crystal MgO to 8 kilobars and 800° K, J. Geophys. Res. 75 (1970) 2073.
16 H.J. McSkimin and P. Andreatch, Jr., Analysis of the pulse superposition method for measuring ultrasonic wave velocities as a function of temperature and pressure, J. Acoust. Soc. Am. 34 (1962) 609.
17 H.J. McSkimin, Ultrasonic measurement techniques applicable to small solid specimens, J. Acoust. Soc. Am. 22 (1950) 413.
18 H.J. McSkimin, Use of high-frequency ultrasound for determining the elastic moduli of small specimens, I.R.E. Trans. on Ultrasonic Engineering PGUE-5 (1957) 25.
19 G.F. Davies and R.J. O'Connell, Transducer and bond phase shifts in ultrasonics, and their effects on measured pressure derivatives of elastic moduli, in: High pressure Research: Applications in Geophysics, M.H. Manghnani and S. Akimoto, eds. (Academic Press, New York, N.Y., 1977).
20 H.J. McSkimin, Pulse superposition method for measuring ultrasonic wave velocities in solids, J. Acoust. Soc. Am. 33 (1961) 12.
21 H.J. McSkimin, P. Andreatch, Jr. and R.N. Thurston, Elastic moduli of quartz versus hydrostatic pressure at 25° and −195.8° C, J. Appl. Phys., 36 (1965) 1624.
22 S. Haussühl, Elastisches und Thermoelastisches Verhalten von MgF_2 und MnF_2, Phys. Status Solidi 28 (1968) 127.
23 K.S. Aleksandrov, L.A. Shabanova and V.I. Zinenko, Elastic constants of MgF_2 single crystals, Phys. Status Solidi 33 (1969) K1.
24 L.E.A. Jones, High-temperature elasticity of rutile-structure MgF_2, Phys. Chem. Miner. (1977) in press.
25 H.R. Cutler, J.J. Gibson and K.A. McCarthy, The elastic constants of magnesium fluoride, Solid State Commun., 6 (1968) 431.
26 Z. Hashin and S. Shtrikman, A variational approach to the theory of the elastic behavior of polycrystals, J. Mech. Phys. Solids 11 (1962) 127.
27 R. Meister and L. Peselnick, Variational method of determining effective elastic moduli of polycrystals with tetragonal symmetry, J. Appl. Phys., 37 (1966) 4121.
28 M. Nicol and M.Y. Fong, Raman spectrum and polymorphism of titanium dioxide at high pressures, J. Chem. Phys. 54 (1971) 3167.
29 G.A. Samara and P.S. Peercy, Pressure and temperature dependence of the static dielectric constants and Raman spectra of TiO_2 (rutile), Phys. Rev. B7 (1973) 1131.
30 I.J. Fritz, Pressure and temperature dependences of the elastic properties of rutile (TiO_2), J. Phys. Chem. Solids 35 (1974) 817.
31 M.E. Striefler and G.R. Barsch, Optical mode gammas, pressure derivatives of elastic and dielectric constants, and stability of rutile-structure fluorides in rigid-ion approximation, Phys. Status Solidi B 64 (1974) 613; correction, 67 (1975) 417.
32 M.E. Striefler and G.R. Barsch, Elastic, optical and dielectric properties and their pressure derivatives of rutile-structure oxides in a modified rigid-ion approximation, Phys. Status Solidi B 67 (1975) 143.
33 H. Wang and G. Simmons, Elasticity of some mantle crystal structures, 2. Rutile GeO_2, J. Geophys. Res. 78 (1973) 1262.
34 M. Manghnani, Elastic constants of single-crystal rutile under pressure to 7.5 kilobars, J. Geophys. Res. 74 (1969) 4317.
35 E. Chang and E.K. Graham, The elastic constants of cassiterite SnO_2 and their pressure and temperature dependence, J. Geophys. Res. 80 (1975) 2595.
36 S. Hart and R.W.H. Stevenson, The elastic compliances of CoF_2, J. Phys. D, Appl. Phys., 3 (1970) 1789.